

# Design and Modeling of 9 Degrees of Freedom Redundant Robotic Manipulator

Zuha Anjum <sup>1\*</sup>, Saifullah Samo <sup>2</sup>, Arbab Nighat <sup>3</sup>, Akhtar Un Nisa <sup>4</sup>, Muhammad Ali Soomro <sup>5</sup>, Reza Alayi <sup>6</sup>

<sup>1, 2, 4, 5</sup> Department of Mechatronic Engineering, Mehran University of Engineering & Technology Jamshoro, Pakistan

<sup>3</sup> Department of Electronics Engineering, Mehran University of Engineering & Technology Jamshoro, Pakistan

<sup>6</sup> Department of Mechanics, Germe Branch, Islamic Azad University, Germe, Iran

Email: <sup>1</sup> zuhaanjum98@gmail.com <sup>2</sup> saifullah.samo@faculty.muett.edu.pk, <sup>3</sup> arbab.nighat@faculty.muett.edu.pk,

<sup>4</sup> 155.15bme@gmail.com, <sup>5</sup> soomro.ali@live.com, <sup>6</sup> reza.alayi@yahoo.com

\* Corresponding Author

**Abstract**—In disaster areas, robot manipulators are used to rescue and clearance of sites. Because of the damaged area, they encounter disturbances like obstacles, and limited workspace to explore the area and to achieve the location of the victims. Increasing the degrees of freedom is required to boost the adaptability of manipulators to avoid disturbances, and to obtain the fast desired position and precise movements of the end-effector. These robot manipulators offer a reliable way to handle the barrier challenges since they can search in places that humans can't reach. In this research paper, the 9-DOF robotic manipulator is designed, and an analytical model is developed to examine the system's behavior in different scenarios. The kinematic and dynamic representation of the proposed model is analyzed to obtain the translation or rotation, and joint torques to achieve the expected position, velocity, and acceleration respectively. The number of degrees may be raised to avoid disturbances, and to obtain the fast desired position and precise movements of the end-effector. The simulation of developed models is performed to ensure the adaptable movement of the manipulators working in distinct configurations and controlling their motion thoroughly and effectively. In the proposed configuration the joints can easily be moved to achieve the desired position of the end-effector and the results are satisfactory. The simulation results show that the redundant manipulator achieves the victim location with various configurations of the manipulator. Results reveal the effectiveness and efficacy of the proposed system.

**Keywords**— *Hyper-Redundant Robotic Manipulator; 9 DOF; Rescue Robot; Cataclysmic; Functional Modeling.*

## I. INTRODUCTION

The manipulators can perform dynamic adaptive manipulation in unstructured situations and are exceptionally dexterous, docile, and flexible. The robot manipulators are being utilized in various forms as rehabilitation robots for dysfunction of the hand [1], for telemetry operations by using quadcopter [2], the dancing robots to be used in competitions in place of humans [3], for the distant operation tasks [4], where the manipulator is used for inspecting the perilous areas or as cleaning robots to wipe the complex industrial territories [5]. Regarding the fatality in the disaster zones, it is needed that manipulators can bend with the proper curvatures and adapt to complicated regions. A redundant manipulator with more than six or more degrees of freedom can alter its configuration while maintaining a fixed position and orientation for its end-effector. Hyper redundant robot

manipulators don't have hard joints like conventional rigid link robots have, and they also have more degrees of freedom, which provide them with some highly beneficial characteristics. It is very difficult in disaster areas to reach every location to rescue the victims with regular robot manipulators due to the unevenness of the ground and obstacles in the way. The most important issues in disaster areas are safety, precision, and robot movement. Various disaster management systems based on microcontrollers are also in consideration [6]. Nowadays robots are widely used in the process of disaster mitigation [7]-[8]. The robots can provide accuracy and precision during the job [9]. The 30 percent of deaths in disasters are due to a lack of timely aid and assistance [10]. With the evolution of technology, robots are being used in almost every field like industries, medical, atomic power plants, search, and rescue operations to ease human tasks and minimize the risks [11]. The proper techniques should be applied so that robots must navigate through simple or complex environments [12]. The manipulators having an extra degree of freedom for a task are known as Hyper Redundant Robotic (HRR) Manipulators. The redundant robots are used to conquer the inadequacies of robots [13]-[14]. These Manipulators have the shape of snakes or tentacles [15].

The most used robotic Manipulators for industries are Serial link manipulators with 6 DOF, manufactured to work like a human arm; comprises of rigid links with a fixed base, and the joints connected through links have motors and gears. The Joint's actuator determines the feasible movement of the manipulator whereas the total torque involves the torque of the motor and torque due to load determines the performance of the joint [16]. There is plenty of advantages of redundant manipulators over 6-DOF manipulators [17]-[22]. The manipulator is designed to achieve target points in the workspace by adjusting the robot joint angles to move the end-effector to the prescribed target [23]. The control schemes are presented to deliver the torque within limits [24]. Robotic arms certainly run into singular configurations during movement resulting in poor performance, thus discerning the singularities is extremely essential [25]. The inexplicit singular configurations and techniques are identified for the 4 DOF and 7 DOF redundant manipulators [26]. Whenever the end-effector reaches a singular point, Robot's motion becomes difficult in a certain direction so, to confront the singularities and to



make the manipulator flexible so that all assigned target points should be achieved by increasing the number of degrees of freedom. The methods to elude the singularity for the co-robots are discussed in [27].

Kinematic modeling using the DH method is used to model 6 DOF manipulators [28]. A 3-DOF small-scale robotic arm is designed for educational purposes and inverse kinematics is applied [29]. The methods to solve inverse kinematics of a redundant manipulator are optimized by fixing the joints [30]-[31]. The DH approach is typically employed in the kinematic modeling of manipulators. Ref. [32] computed kinematics through the Denavit Hartenberg method on LabVIEW. The paper [33] implemented a real-time configured kinematics of 9 DOF surgical robot, using a decision maker to auto-select the specific movements, control, and speed as per the velocity of tactual device. In [34], Denavit Hartenberg analysis of the forward and inverse kinematics of 5 and 6 DOF manipulators was performed. In [35], evaluated the kinematics and workspace of the designed 6 DOF manipulator. Typically, the Lagrange-Euler equation is employed to derive the dynamic model of the manipulators. Ref. [36] used the Lagrange-Euler technique to derive the dynamic modeling of a 2-DOF manipulator. In [37], designed a system of controlled Robotic arm on wheelchair containing 7-DOF arm with 2-DOF control of wheelchair for the disabled people. In paper [38], using AutoCAD and MATLAB as testing tools, Kinematics, path planning, and Jacobian velocities were evaluated in an AL5B Educational Robot. This study [39] combined two distinct approaches that are axis-invariant and dual quaternions for the location and orientation of the end-effector with the least amount of error to simulate the inverse kinematics for the 6 DOF manipulator. The paper [40] presented a 7-DOF humanoid robotic arm with a configuration like a human arm. To get the inverse solution of the humanoid robotic arm, an integrated approach and optimization of the arm angle technique were proposed. Accurate trajectory tracking is a key component in the design of position control for robot manipulators since robot manipulators have complex dynamics and are impacted by large uncertainties and outside disturbances. This paper [41] developed an extended state observer-based position control system for a robot manipulator. The DH approach was utilized to determine the forward kinematics of a 6 DOF manipulator model for flat welding movement, while geometric and algebraic methods were employed to calculate the inverse kinematics. Through the LSPB (linear segment parabolic bend) approach, trajectory tracking was performed [42].

Hyper redundant manipulators are ideal candidates for optimization methods because they can avoid obstructions and singularities. Because of their great ability to avoid obstacles, hyper-redundant manipulators made of numerous serially connected short links are effective in challenging and constrained environments like disaster zones, nuclear or chemical plants, and space stations. The earlier studies lack considering the hyper-redundant manipulators to be implemented in catastrophic areas, most of the studies examine employing them in the industrial or medical fields, whereas to outreach sufferers the proposed model by

variegated configurations can be exerted by progressing through the asymmetrical path.

In this study, limitations of less DOF robotic manipulators, such as singularities which occur whenever the two axes of the robot manipulator become parallel and the manipulator cannot achieve the aim position, a constrained work area that is imposed on a robotic system that reduces the range of motion that it is capable of, and the joint limit specifying the amount of motion that rotating parts of an assembly are permitted to undergo are overcome. Thus, by raising the number of degrees of the manipulator, redundancy is included to improve performance in challenging circumstances. A requirement for upcoming contemporary and unmanned industries, manipulator performance must be able to deliver flexible and efficient fabrication. The research contribution is to develop a model of a redundant robot manipulator with 9 degrees of freedom that can avoid obstructions, and singularities and can help to search the victim's position by using redundancy. It can function in confined spaces, reach unstructured circumstances, and navigate through environments with a high density of obstacles.

## II. ANALYSIS OF ROBOT KINEMATICS

### A. Kinematic Modeling

There should be no forces or torques in the kinematic model for the 9 DOF HRR Manipulator. To obtain the location and orientation of the end-effector, the kinematic modeling is solved using the Denavit- Hartenberg method. The first step in the DH technique is to give the joints coordinate frames to show how the end-effector is oriented and where it is about the base. Seven revolute joints and two prismatic joints are part of the 9-DOF manipulator model that is being exhibited. The joints are designated as  $\Theta_i$  and Table-I contains the DH table for resolving the manipulator's kinematics in the homing position. The Denavit- Hartenberg convention is used to get the Homogenous Transformation Matrix [43].

TABLE I. 9-LINK DH PARAMETER TABLE

Joints	$\theta_i$ ( $^\circ$ )	$d_i$ (mm)	$a_i$ (mm)	$\alpha$ ( $^\circ$ )
(0-1)1	$\theta_1$	0	$a_2$	$90^0$
(1-2) 2	$\theta_2 + 90^0$	0	$a_3$	$90^0$
(2-3) 3	$\theta_3$	0	$a_4$	$90^0$
(3-4) 4	$\theta_4$	0	0	0
(4-5) 5	$90^0$	0	$a_5 + a_6 + d_5$	0
(5-6) 6	$\theta_6 - 90^0$	0	$a_7$	$-90^0$
(6-7) 7	$\theta_7$	0	0	$90^0$
(7-8) 8	$90^0$	0	$a_8 + a_9 + d_8$	0
(8-9) 9	$\theta_9$	0	$a_{10}$	0

The link function in the Robotics toolbox is used to map the link object containing details for one axis, Function named Serial-link gathers every link object and generates the manipulator. A 9 DOF Robotic manipulator at homing position is shown in Fig. 1 where the joints are stretched to their fullest possessing a configuration

$$R_1 \perp R_2 \perp R_3 \perp R_4 \perp P_5 \parallel R_6 \perp R_7 \perp P_8 \parallel R_9$$

Where P and R show Prismatic and Revolute joints respectively.

In Fig. 2, the manipulator is in a random position whose  $P_5 \perp R_6 \perp R_7$ . While in Fig. 3 the pattern changes and  $R_1 \perp R_2 \parallel R_3$ . The configuration of Fig. 4 shows  $P_5$  becomes orthogonal to  $R_6$ . In Fig. 5, the arrangement of the joints to penetrate atypical domains can be seen whose  $R_1$  and  $R_2$  are orthogonal to each other, and the joints are at various angles. Similarly, Fig. 6 also demonstrates the configuration for peculiar environs where

$$R_1 \perp R_2 \perp R_3 \perp R_4 \perp P_5 \parallel R_6 \perp R_7 \perp P_8 \perp R_9$$

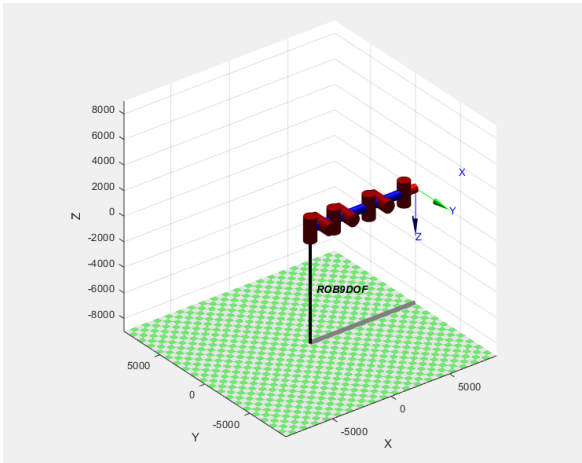


Fig. 1. 09 joint Redundant manipulator at Homing Position.

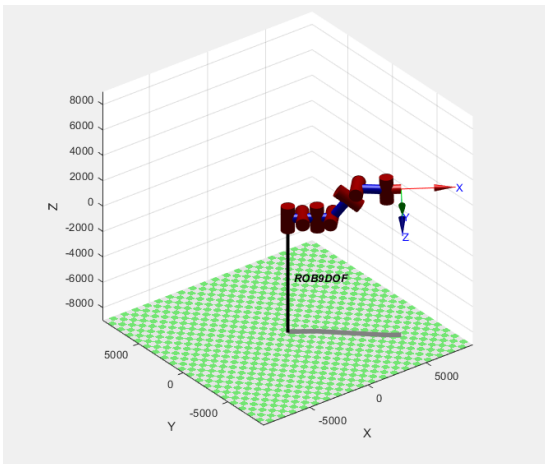


Fig. 2. 09 joint manipulator at Random configuration-A

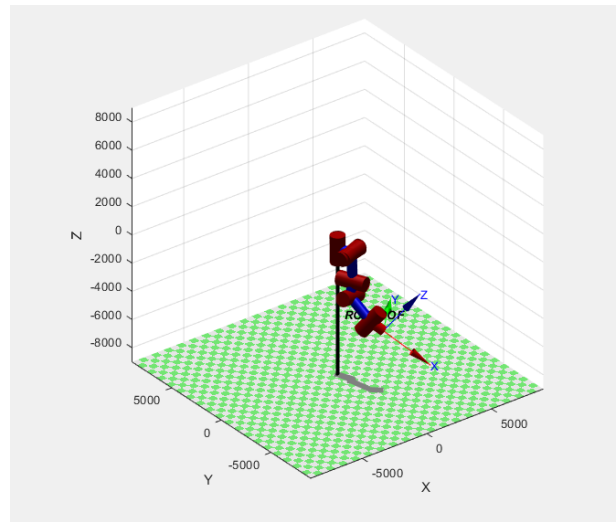


Fig. 3. 09 joint manipulator at Random configuration-B

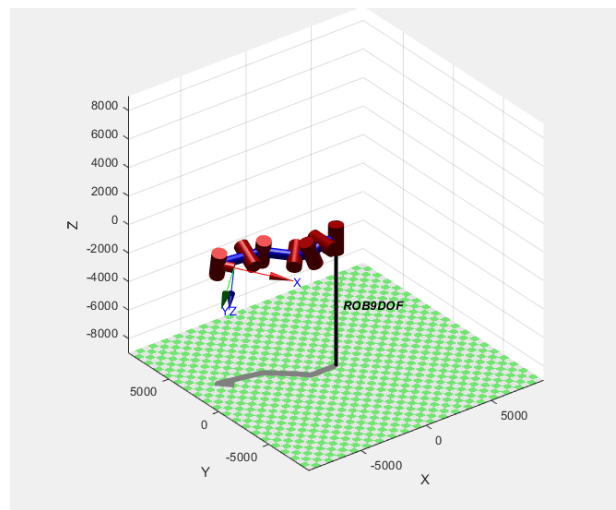


Fig. 4. 09 joint manipulator at Random configuration-C

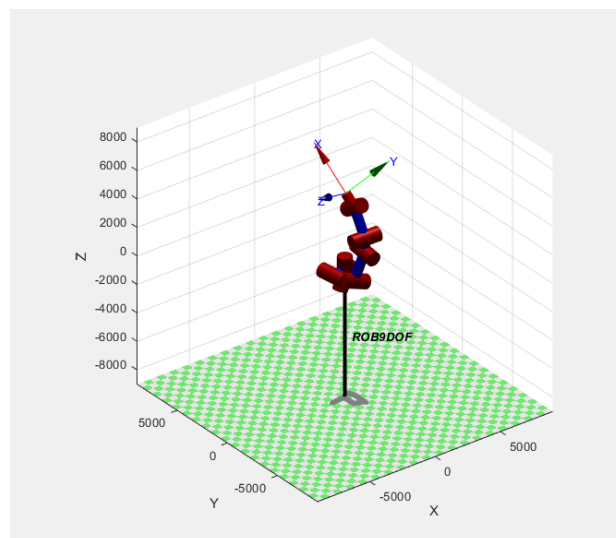


Fig. 5. 09 joint manipulator at Random configuration-D

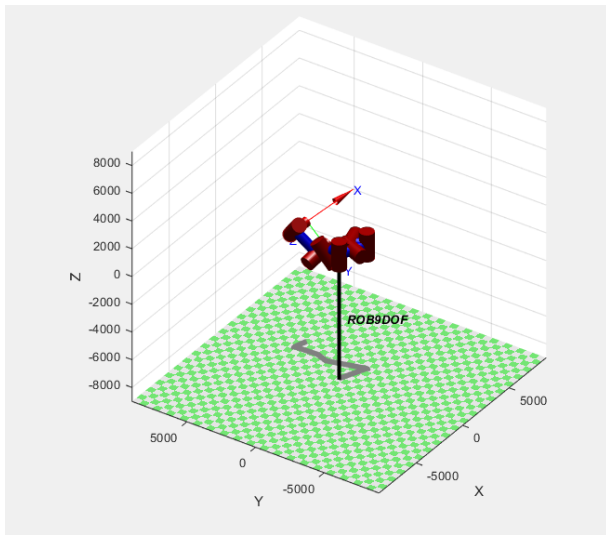


Fig. 6. 09 joint manipulator at Random configuration-E

The forward kinematics is to be calculated to realize the accumulative impact of all joint variables on the end-effector and is analyzed through homogenous transformation given as in Equation (1), where  $c$  denotes the cos angle,  $s$  shows the angle of sin and  $a_n$  illustrates the respective link lengths. The Homogenous matrix for revolute joint 1 can be seen in Equation (2). To ascertain the total impact on the end-effector, the homogeneous transformation for each individual joint must be found. The second revolute Joint matrix is shown in Equation (3). Equation (4) depicts the homogenous transformation for the third joint. For the fourth revolute joint, the matrix is given as in Equation (5). The fifth joint is prismatic, Equation (6) is its homogenous matrix. Equation (7) shows the sixth joint homogenous matrix, where the matrix for the 7<sup>th</sup> joint is given in Equation (8). Equation (9) and (10) delineates the homogenous matrix for joint 8<sup>th</sup> and 9<sup>th</sup> respectively.

$$H_n^0 = \begin{bmatrix} c(\Theta n) & -s(\Theta n) c(\alpha n) & s(\Theta n) \sin(\alpha n) & a_n * c(\Theta n) \\ s(\Theta n) & c(\Theta n) c(\alpha n) & -c(\alpha n) \sin(\Theta n) & a_n * s(\Theta n) \\ 0 & s(\alpha n) & c(\alpha n) & d_n \\ 0 & 0 & 0 & 1 \end{bmatrix} \quad (1)$$

$$H_0^1 = \begin{bmatrix} C1 & 0 & -S1 & a_1 * C1 \\ S1 & 0 & C1 & a_1 * S1 \\ 0 & -1 & 0 & 0 \\ 0 & 0 & 0 & 1 \end{bmatrix} \quad (2)$$

$$H_1^2 = \begin{bmatrix} C2 & 0 & -S2 & a_2 * C2 \\ S2 & 0 & C2 & a_2 * S2 \\ 0 & -1 & 0 & 0 \\ 0 & 0 & 0 & 1 \end{bmatrix} \quad (3)$$

$$H_2^3 = \begin{bmatrix} C3 & 0 & S3 & a_3 * C3 \\ S3 & 0 & -C3 & a_3 * S3 \\ 0 & 1 & 0 & 0 \\ 0 & 0 & 0 & 1 \end{bmatrix} \quad (4)$$

$$H_3^4 = \begin{bmatrix} C4 & 0 & -S4 & 0 \\ S4 & 0 & C4 & 0 \\ 0 & -1 & 0 & 0 \\ 0 & 0 & 0 & 1 \end{bmatrix} \quad (5)$$

$$H_4^5 = \begin{bmatrix} 1 & 0 & 0 & a_5 + a_6 \\ 0 & 1 & 0 & 0 \\ 0 & 0 & 1 & 0 \\ 0 & 0 & 0 & 1 \end{bmatrix} \quad (6)$$

$$H_5^6 = \begin{bmatrix} C6 & 0 & S6 & a_7 * C6 \\ S6 & 0 & -C6 & a_7 * S6 \\ 0 & 1 & 0 & 0 \\ 0 & 0 & 0 & 1 \end{bmatrix} \quad (7)$$

$$H_6^7 = \begin{bmatrix} C7 & 0 & -S7 & 0 \\ S7 & 0 & C7 & 0 \\ 0 & -1 & 0 & 0 \\ 0 & 0 & 0 & 1 \end{bmatrix} \quad (8)$$

$$H_7^8 = \begin{bmatrix} 1 & 0 & 0 & a_8 + a_9 \\ 0 & 1 & 0 & 0 \\ 0 & 0 & 1 & 0 \\ 0 & 0 & 0 & 1 \end{bmatrix} \quad (9)$$

$$H_8^9 = \begin{bmatrix} C9 & -S9 & 0 & a_{10} * C9 \\ S9 & C9 & 0 & a_{10} * S9 \\ 0 & 0 & 1 & 0 \\ 0 & 0 & 0 & 1 \end{bmatrix} \quad (10)$$

To determine the cumulative influence of all joint variables on the end-effector, the forward kinematics must be determined. This analysis is done using the homogeneous transformation given in (11).

$$H_0^n = \begin{bmatrix} n_x & o_x & a_x & P_x \\ n_y & o_y & a_y & P_y \\ n_z & o_z & a_z & P_z \\ 0 & 0 & 0 & 1 \end{bmatrix} \quad (11)$$

Links that connect the joints in a robotic arm model have precise values that allow the arm to move to different distances. The link length values are taken from Table II, where  $d_5$  and  $d_8$  represent prismatic links and the other links, numbered from  $a_1$  to  $a_{10}$ , revolute joints.

TABLE II. LINK LENGTHS

Joints	a1	a2	a3	a4	d5	a6	a7	d8	a9	a10
Length (m)	0.4	0.4	0.4	0.4	0.4	0.4	0.4	0.4	0.4	0.4

It is determined that the homogenous matrix  $H_f$  for the manipulator displaying the end effector's orientation and the location at homing position is illustrated in (12).

$$H_f = \begin{bmatrix} 1.000 & 0 & 0 & 5.2000 \\ 0 & -1.000 & 0 & 0 \\ 0 & 0 & -1.000 & 0 \\ 0 & 0 & 0 & 1.000 \end{bmatrix} \quad (12)$$

The forward kinematic matrix for the designed manipulator is given in (13).

### B. Dynamic Modeling

Dynamic modeling considers the forces and torques modifying the system. The difference between the potential and kinetic energy can be used to represent the dynamic system and to calculate the forward dynamics and inverse dynamics using the Euler-Lagrange Approach. The dynamic model that is used the most is delineated in (14).



The angular positions ( $^{\circ}$ ) of all the nine joints are depicted in Fig. 17 and  $q$  shows the joint number. The angular velocities ( $^{\circ}/s$ ) are displayed in Fig. 18 while the angular accelerations ( $^{\circ}/s^2$ ) are plotted in Fig. 19. Fig. 20 describes the torque required for each joint to move the manipulator to the target point.

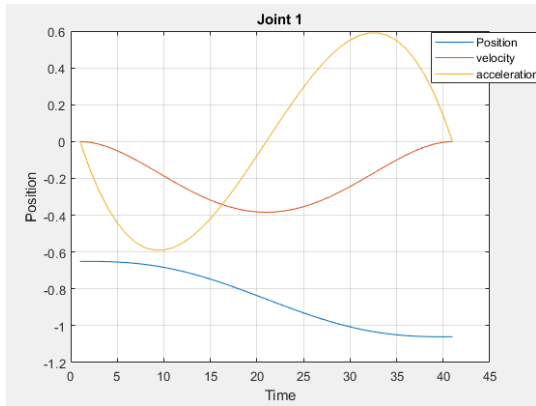


Fig. 8. Plot for joint 1

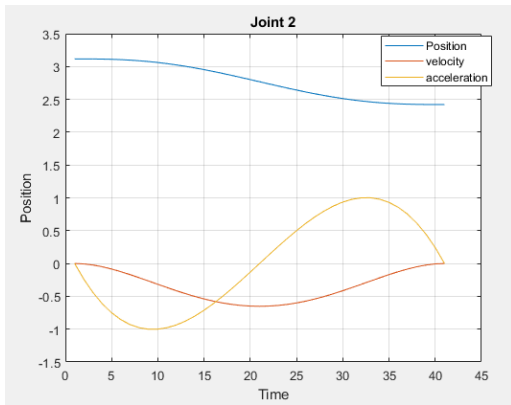


Fig. 9. Plot for joint 2

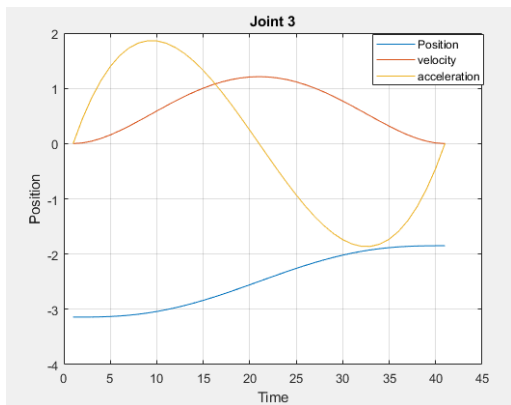


Fig. 10. Plot for joint 3

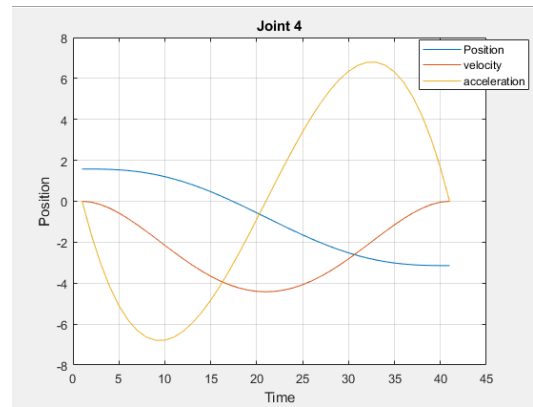


Fig. 11. Plot for joint 4

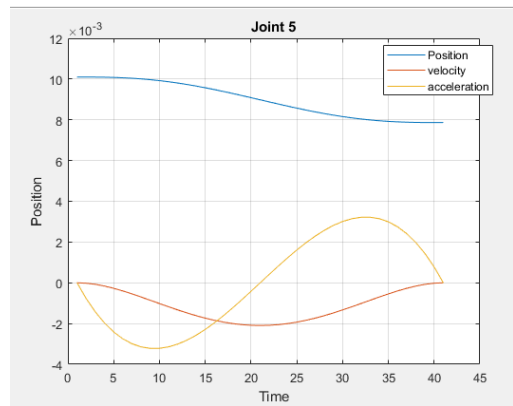


Fig. 12. Plot for joint 5

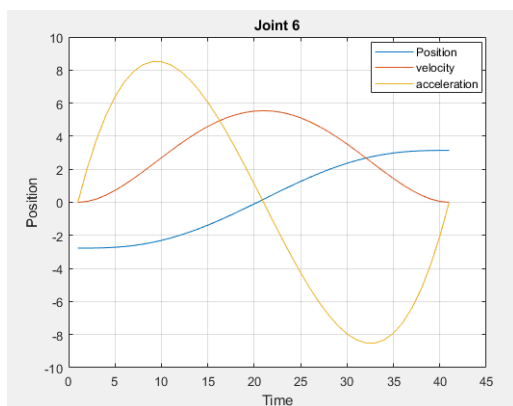


Fig. 13. Plot for joint 6

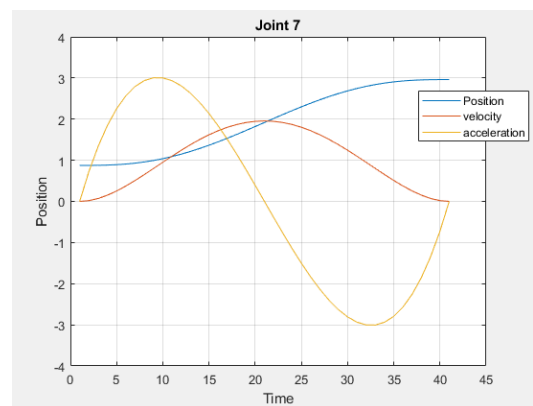


Fig. 14. Plot for joint 7

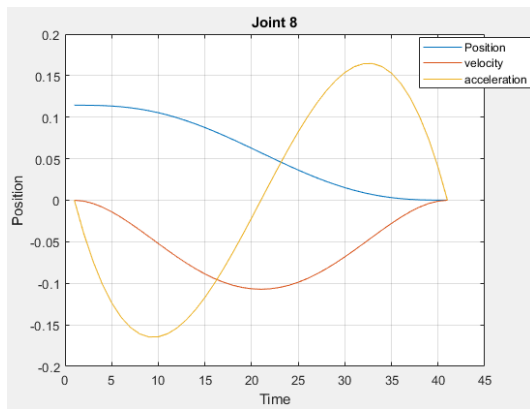


Fig. 15. Plot for joint 8

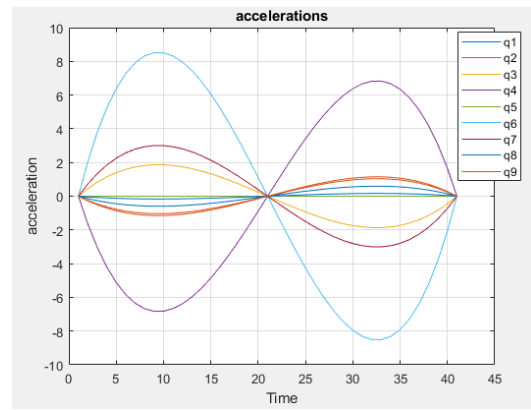


Fig. 19. Accelerations plot for 9-Joints.

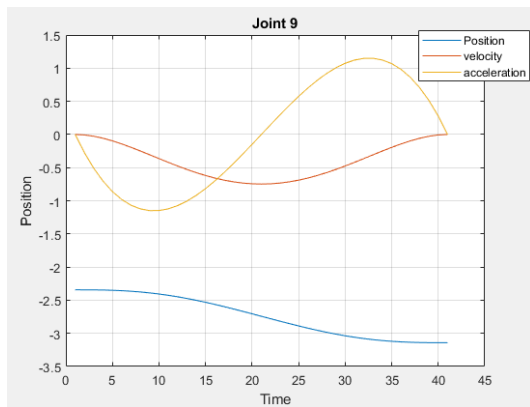


Fig. 16. Plot for joint 9

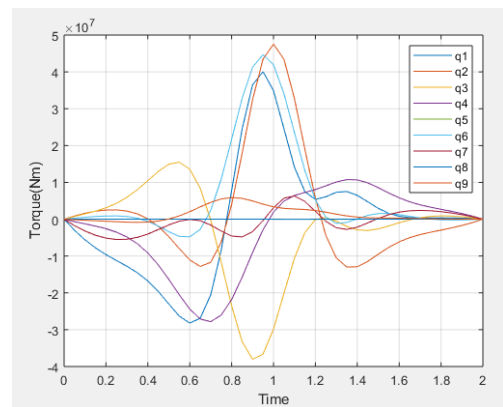


Fig. 20. Plot for 9-Joints torques

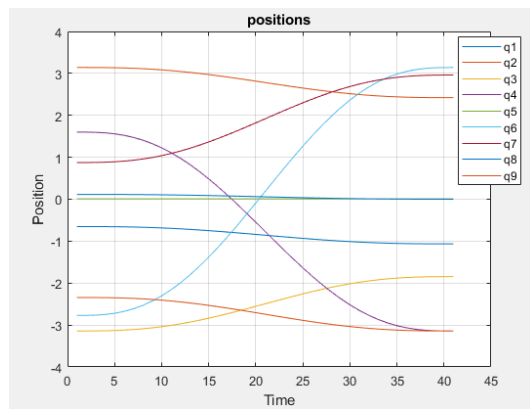


Fig. 17. Positions of 9-Joints.

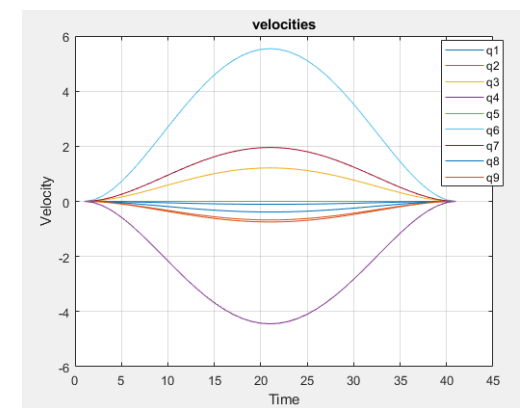


Fig. 18. Velocities plot for 9-Joints.

#### IV. CONCLUSION AND FUTURE RECOMMENDATIONS

The proposed configuration of a 9 DOF (4RP2RPR) robotic manipulator has been modeled in this study. The work determined the dynamic and kinematic modeling of the manipulator. The designed model can be used in disastrous places, where the manipulator can achieve complex shapes circumventing barriers, to enter the holes or sides of walls intending to reach the target points. The Model shows precise angles of joints to move the manipulator's end-effector to the required position. The velocities and accelerations are plotted by the quintic approach. Torques required for each joint are plotted to move the manipulator to the goal position. The evaluated results show an effective and appropriate approach to be implemented practically. The study can further be advanced by applying the inverse kinematics with the controller to the manipulator and indicating the realistic tracks of the destructive domain to get the objectives with minimum error and improved efficiency.

#### ACKNOWLEDGMENT

The authors are highly grateful to Mehran University of Engineering & Technology, Jamshoro, Pakistan for the support, necessary laboratory facilities, and comfortable research environment.

#### REFERENCES

[1] X. Zhu and B. He, "Underactuated Rehabilitation Robotics for Hand Function," *Journal of Robotics and Control (JRC)*, vol. 2, no. 5, pp. 337-341, 2021, <https://doi.org/10.18196/jrc.25103>.

- [2] M. I. F. Hatta and N. S. Widodo, "Robot Operating System (ROS) in Quadcopter Flying Robot Using Telemetry System," *International Journal of Robotics and Control Systems*, vol. 1, no. 1, pp. 54–65, 2021, <https://doi.org/10.31763/ijrcs.v1i1.247>
- [3] I. Rifajar and A. Fadlil, "The Path Direction Control System for Lanange Jagad Dance Robot Using the MPU6050 Gyroscope Sensor," *International Journal of Robotics and Control Systems*, vol. 1, no. 1, pp. 27–40, 2021, <https://doi.org/10.31763/ijrcs.v1i1.225>
- [4] Martín-Barrio, Andrés, et al. "Design of a Hyper-Redundant Robot and Teleoperation Using Mixed Reality for Inspection Tasks," *Sensors*, vol. 20, no. 8, p. 2181, 2020 <https://doi.org/10.3390/s20082181>.
- [5] B. Hao, H. Du, X. Dai, and H. Liang, "Automatic Recharging Path Planning for Cleaning Robots," *Mobile Information Systems*, vol. 2021, 2021, <https://doi.org/10.1155/2021/5558096>
- [6] A. A. Beltran Jr, K. J. T. Dizon, K. C. Nones, R. L. M. Salanguit, J. B. D. Santos, J. R. G. Santos, "Arduino-based Disaster Management Alarm System with SMS," *Journal of Robotics and Control (JRC)*, vol. 2, no. 1, pp. 24-28, 2022, <https://doi.org/10.18196/jrc.2147>.
- [7] S. Shan, F. Zhao, Y. Wei, M. Liu, "Disaster management 2.0: A real-time disaster damage assessment model based on mobile social media data—A case study of Weibo (Chinese Twitter)," *Safety Science*, vol. 201, 2019.
- [8] C. Mouradian, S. Yangui, R.H. Glitho, "Robots as-a-service in cloud computing: Search and rescue in large-scale disasters case study," *15th IEEE Annual Consumer Communications Networking Conference (CCNC)*, p. 1–7, 2018.
- [9] M. Marsono, Y. Yoto, A. Suyetno, R. Nurmalasari, "Design and Programming of 5 Axis Manipulator Robot with GrblGru Open Source Software on Preparing Vocational Students' Robotic Skills," *Journal of Robotics and Control (JRC)*, vol. 2, no. 1, pp. 539-545. 2021, <https://doi.org/10.18196/jrc.26134>.
- [10] J. R. Deng, "Research on Rescue Robot Model Design," *Industry and Technology Forum*, vol. 17, no. 2, pp. 36-37, 2018.
- [11] A. Wolf et al., "A Mobile Hyper Redundant Mechanism for Search and Rescue Tasks," *IEEE Int. Conf. Intell. Robot. Syst.*, vol. 3, pp. 2889–2895, 2003.
- [12] I. Hassani, I. Ergui, and C. Rekik, "Turning Point and Free Segments Strategies for Navigation of Wheeled Mobile Robot," *International Journal of Robotics and Control Systems*, vol. 2, no. 1, pp.172-186. 2022, <https://doi.org/10.31763/ijrcs.v2i1.586>.
- [13] J. J. Duan, Y. H. Gan, X. Z. Dai et al., "Inverse solution method of redundant robot based on operability evaluation," *Journal of Huazhong University of science and Technology (Natural Science Edition)*, vol. 57, no. z1, pp. 45-48, 2015
- [14] S. Mukai and N. Maru, "Redundant Arm Control by Linear Visual Servoing Using Pseudo Inverse Matrix," *2006 IEEE/RSJ International Conference on Intelligent Robots and Systems*, pp. 1237-1242, 2006.
- [15] R. T. Sataloff, M. M. Johns, and K. M. Kost, "Hyper-Redundant Robot Mechanisms and Their Applications," *IEEE/RSJ International Workshop on intelligent Robots and systems*, 1991
- [16] E. C. Agbaraji, H. C. Inyama, and I. Obiora-dimson, "Joint Torque and Motion Computational Analysis for Robotic Manipulator Arm Design," *Journal of Engineering and Applied Sciences*, vol. 12, pp. 1–9, 2018.
- [17] P. K. Patchaikani, L. Behera and G. Prasad, "A single network adaptive critic-based redundancy resolution scheme for robot manipulators," *IEEE Trans. Ind. Electron.*, vol. 59, pp. 3241-3253, Aug. 2012.
- [18] D. N. Nenchev, Y. Tsumaki and M. Takahashi, "Singularity-consistent kinematic redundancy resolution for the S-R-S manipulator," *Proc. IEEE/RSJ Int. Conf. Intell. Robots Syst.*, Apr. 2004.
- [19] M. M. Schill and M. Buss, "Kinematic trajectory planning for dynamically unconstrained nonprehensile joints," *IEEE Robot. Autom. Lett.*, vol. 3, no. 2, pp. 728-734, Apr. 2018.
- [20] A. Flores-Abad, O. Ma, K. Pham and S. Ulrich, "A review of space robotics technologies for on-orbit servicing," *Prog. Aerosp. Sci.*, vol. 68, no. 8, pp. 1-26, Jul. 2014.
- [21] H. Kim, L. M. Miller, N. Byl, G. Abrams and J. Rosen, "Redundancy resolution of the human arm and an upper limb exoskeleton," *IEEE Trans. Biomed. Eng.*, vol. 59, no. 6, pp. 1770-1779, Jun. 2012.
- [22] P. Berthet-Rayne, K. Leibrandt, G. Gras, P. Fraitse, A. Crosnier and G.-Z. Yang, "Inverse kinematics control methods for redundant snakelike robot teleoperation during minimally invasive surgery," *IEEE Robot. Autom. Lett.*, vol. 3, no. 3, pp. 2501-2508, Jul. 2018.
- [23] J. Zhang, Q. Meng, X. Feng, and H. Shen, "A 6 - DOF robot - time optimal trajectory planning based on an improved genetic algorithm," *Robot. Biomimetics*, pp. 3–9, 2018.
- [24] B. S. García, F. R. Cortés, B.M. Al-Hadithi, O. F. Beltrán, "Global Saturated Regulator with Variable Gains for Robot Manipulators", *International Journal of Robotics and Control*, vol.02, no.06, pp.24-28. 2022. <https://doi.org/10.18196/jrc.26139>.
- [25] X. Zhang, B. Fan, C. Wang, and X. Cheng, "Analysis of Singular Configuration of Robotic Manipulators," *Electronics*, vol. 10, no. 18, p. 2189, 2021.
- [26] A. A. Almarkhi and A. A. Maciejewski, "Singularity analysis for redundant manipulators of arbitrary kinematic structure," *ICINCO 2019 - Proc. 16th Int. Conf. Informatics Control. Autom. Robot.*, vol. 2, pp. 42–49, 2019, <https://doi.org/10.5220/0007833100420049>.
- [27] Wang H, Zhou Z, Zhong X, Chen Q. "Singular Configuration Analysis and Singularity Avoidance with Application in an Intelligent Robotic Manipulator," *Sensors*, vol. 22, no. 3, p. 1239, 2022, <https://doi.org/10.3390/s22031239>.
- [28] S. A. Ajwad, J. Iqbal, R. U. Islam, A. Alsheikhy, A. Almeshal, and A. Mehmood, "Optimal and Robust Control of Multi DOF Robotic Manipulator: Design and Hardware Realization," *Cybern. Syst.*, vol. 49, no. 1, pp. 77–93, 2018.
- [29] A. R. A. Tahtawi, M. Agni and T. D. Hendrawati, "Small-scale Robot Arm Design with Pick and Place Mission Based on Inverse Kinematics," *Journal of Robotics and Control*, vol. 2, pp. 469–475, 2021, <https://doi.org/10.18196/jrc.26124>.
- [30] Y. Chen, Y. Chen, and J. Guo, "An optimization algorithm to expand the reduced workspace with fixed-joint method for redundant manipulator," in *2016 IEEE Workshop on Advanced Robotics and its Social Impacts (ARSO)*, pp. 116–120, July 2016
- [31] I. Zaplana and L. Basanez, "A novel closed-form solution for the inverse kinematics of redundant manipulators through workspace analysis," *Mechanism and Machine Theory*, vol. 121, pp. 829–843, March 2018.
- [32] H. A. R. Akkar and A. Najim, "Forward Kinematics and Workspace Analysis of 6DOF Manipulator Arm Applied on Lab VIEW," *Saussurea*, vol. 7, no. 1, pp. 1-11, 2017.
- [33] B. Sunal, E. Oztop, and O. Bebek, "Adaptive Inverse Kinematics of a 9-DOF Surgical Robot for Effective Manipulation," *2019 4th IEEE Int. Conf. Adv. Robot. Mechatronics, ICARM 2019*, pp. 678–683, 2019.
- [34] T. P. Singh, P. Suresh, and S. Chandan, "Forward and Inverse Kinematic Analysis of Robotic Manipulators," *International Research Journal of Engineering and Technology (IRJET)*, vol. 4, no. 2, pp. 1459-1468, 2017.
- [35] J. Iqbal, R. Islam, and H. Khan, "Modeling and Analysis of a 6 DOF Robotic Arm Manipulator," *Canadian Journal on Electrical and Electronics Engineering*, vol. 3, no. 6, pp. 300-306, 2012.
- [36] M. Hüseyinoğlu and T. Abut, "Dynamic model and control of 2-dof robotic arm," *European Journal of Technique (EJT)*, vol. 8, no. 2, pp. 141-150, 2018.

- [37] M. Palankar *et al.*, "Control of a 9-DoF wheelchair-mounted robotic arm system using a P300 brain computer interface: Initial experiments," *2008 IEEE Int. Conf. Robot. Biomimetics, ROBIO 2008*, pp. 348–353, 2009.
- [38] M. A. Qassem, I. M. Abuhadrous, and H. Elaydi, "Modeling and Simulation of 5 DOF educational robot arm," *2010 2nd International Conference on Advanced Computer Control*, pp. 569–574, 2010.
- [39] A. Ahmed, M. Yu, and F. Chen, "Inverse Kinematic Solution of 6-DOF Robot-Arm Based on Dual Quaternions and Axis Invariant Methods," *Arab. J. Sci. Eng.*, 2022.
- [40] R. Dou *et al.*, "Inverse kinematics for a 7-DOF humanoid robotic arm with joint limit and end pose coupling," *Mech. Mach. Theory*, vol. 169, no. September 2021, p. 104637, 2022.
- [41] S. J. Abbasi, H. Khan, J. W. Lee, M. Salman, and M. C. Lee, "Robust Control Design for Accurate Trajectory Tracking of Multi-Degree-of-Freedom Robot Manipulator in Virtual Simulator," *IEEE Access*, vol. 10, pp. 17155–17168, 2022.
- [42] M. A. N. Huda, S. H. Susilo, and P. M. Adhi, "Implementation of Inverse Kinematic and Trajectory Planning on 6-DOF Robotic Arm for Straight-Flat Welding Movement," *Log. J. Ranc. Bangun dan Teknol.*, vol. 22, no. 1, pp. 51–61, 2022.
- [43] J. Cashbaugh and C. Kitts, "Automatic calculation of a transformation matrix between two frames," *IEEE Access*, vol. 6, pp. 9614–9622, 2018.
- [44] C. Ji, M. Kong and R. Li, "Time-energy optimal trajectory planning for variable stiffness actuated robot," *IEEE Access*, vol. 7, pp. 14366–14377, 2019.
- [45] X. Lv, Z. Yu, M. Liu, G. Zhang and L. Zhang, "Direct trajectory planning method based on IEPPO and fuzzy rewards and punishment theory for multi-degree-of freedom manipulators," *IEEE Access*, vol. 7, pp. 20452–20461, 2019.
- [46] X. Zhang, Y. Fang and N. Sun, "Minimum-time trajectory planning for underactuated overhead crane systems with state and control constraints," *IEEE Trans. Ind. Electron.*, vol. 61, pp. 6915–6925, Dec. 2014.
- [47] Y. Liu, M. Cong, H. Dong and D. Liu, "Reinforcement learning and EGA-based trajectory planning for dual robots," *Int. J. Robot. Automat.*, vol. 33, no. 4, pp. 367–378, 2018.
- [48] A. Gasparetto and V. Zanotto, "A new method for smooth trajectory planning of robot manipulators," *Mech. Mach. Theory*, vol. 42, no. 4, pp. 455–471, 2007.
- [49] S. Kucuk, "Optimal trajectory generation algorithm for serial and parallel manipulators," *Robot. Comput.-Integr. Manuf.*, vol. 48, pp. 219–232, Dec. 2017.
- [50] M. Q. Mohammed, M. F. Miskon, M. B. Bin, and S. A. Ali, "Comparative Study Between Quintic and Cubic Polynomial Equations Based Walking Trajectory of Exoskeleton System," *International Journal of Mechanical & Mechatronics Engineering*, vol. 17, no. 4, 2017.
- [51] R. Roy, M. Mahadevappa and C. S. Kumar, "Trajectory path planning of EEG controlled robotic arm using GA," *Procedia Comput. Sci.*, vol. 84, pp. 147–151, Dec. 2016.
- [52] L. Tian and C. Collins, "An effective robot trajectory planning method using a genetic algorithm," *Mechatronics*, vol. 14, no. 5, pp. 455–470, Jun. 2004.
- [53] H.-I. Lin, "A fast and unified method to find a minimum-jerk robot joint trajectory using particle swarm optimization," *J. Intell. Robot. Syst.*, vol. 75, no. 3, pp. 379–392, 2014.
- [54] M. Wang, J. Luo and U. Walter, "Trajectory planning of free-floating space robot using particle swarm optimization (PSO)," *Acta Astronautica*, vol. 112, pp. 77–88, Jul./Aug. 2015.
- [55] S. Kucuk, "Energy minimization for 3-RRR fully planar parallel manipulator using particle swarm optimization," *Mech. Mach. Theory*, vol. 62, pp. 129–149, Apr. 2013.
- [56] Z. Qingzhen, G. Chen, G. Fei and R. Zhang, "Reentry trajectory planning optimization based on sequential quadratic programming," *Proc. 2nd Int. Symp. Syst. Control Aerosp. Astronaut.*, vol. 1, pp. 1–5, Dec. 2008.
- [57] A. Gasparetto and V. Zanotto, "A technique for time-jerk optimal planning of robot trajectories," *Robot. Comput.-Integr. Manuf.*, vol. 24, no. 3, pp. 415–426, 2008.